

Attosecond Electron Bunches

N. Naumova,^{1,*} I. Sokolov,² J. Nees,¹ A. Maksimchuk,¹ V. Yanovsky,¹ and G. Mourou¹

¹Center for Ultrafast Optical Science and FOCUS Center, University of Michigan, Ann Arbor, Michigan 48109, USA

²Space Physics Research Laboratory, University of Michigan, Ann Arbor, Michigan 48109, USA

(Received 21 April 2004; published 4 November 2004)

Electron bunches of attosecond duration may coherently interact with laser beams. We show how p -polarized ultraintense laser pulses interacting with sharp boundaries of overdense plasmas can produce such bunches. Particle-in-cell simulations demonstrate attosecond bunch generation during pulse propagation through a thin channel or in the course of grazing incidence on a plasma layer. In the plasma, due to the self-intersection of electron trajectories, electron concentration is abruptly peaked. A group of counterstream electrons is pushed away from the plasma through nulls in the electromagnetic field, having inherited a peaked electron density distribution and forming relativistic ultrashort bunches in vacuum.

DOI: 10.1103/PhysRevLett.93.195003

PACS numbers: 52.38.Kd, 52.27.Ny, 52.65.Rr

The attosecond temporal domain is of interest, not only for studies of atomic and molecular dynamics [1], but also for the generation of high fields and coherent x rays. We have previously shown how electromagnetic pulses of attosecond duration can be formed by a laser pulse that self-organizes its own reflection from an overdense plasma [2]. In that work, the short interaction length imposed by the overdense plasma fostered fine structure in the resulting radiation. Indeed, this effect is so efficient that it could be applied to bring us close to the critical field, which bears electron-positron pairs from vacuum, because the attosecond pulses could, in principle, be focused to a much smaller spot [3]. Experimentally, with the reduction of the focal volume of the laser pulse [4], a highly relativistic intensity of 10^{22} W/cm² has been achieved [5], with 0.8- μ m 30-fs laser pulses focused to a 0.8- μ m diameter spot. Here we demonstrate that a relativistically strong ($a_0 = eE_0/m_e\omega_0c > 1$) tightly focused short laser pulse can, interacting with an overdense plasma, generate electron bunches of attosecond duration. These bunches could be applied to plasma wakefield acceleration, attosecond electron diffraction and microscopy, and, via Thomson scattering, to coherent x-ray production and radiography.

Laser-plasma interactions that drive electrons in overdense plasmas have been extensively investigated theoretically and experimentally (see the review in Ref. [6]). Recently electron jets have been directly observed in experiments during the interaction of p -polarized laser pulses with solid targets [7], and indirect evidence for the same effect (jetlike x-ray emission) has been obtained with s -polarized laser pulses [8] as well. Collimated electron jets for both polarizations have been observed in simulations of overdense plasma [9–11]. Evidence of ultrashort electron bunches has been found experimentally at the rear surface of thick solid targets [12]. The electron *ejection* was assigned to either vacuum or $j \times B$ heating mechanisms [13,14], and their *collimation* to self-generated quasistatic magnetic fields [15]; however, the

details of electron *bunching* were not given by these authors.

In this Letter we discuss the conditions that are required for efficient backward Thomson scattering and we demonstrate in detail, with the help of particle-in-cell (PIC) simulations, how overdense plasmas, reflecting relativistically intense tightly focused ultrashort pulses, become sources of freely propagating attosecond electron bunches. We also show the high conversion efficiency of grazing incidence p -polarized laser pulses impinging on overdense plasmas to attosecond electron bunches and attosecond electromagnetic pulses.

Let us consider an electron beam interacting with a powerful electromagnetic wave. Among different kinds of interaction is Thomson scattering, which can convert the powerful laser wave to a highly collimated x-ray beam [16]. Straightforward estimates result in the evident considerations, that the efficiency of this interaction crucially depends on the ability to form the said electron beam into electron bunches, and that, for this interaction to be coherent, the bunch thickness, d , in the direction of the electron propagation should be much less than the wavelength, λ , of the electromagnetic wave (i.e., their duration should be in the attosecond range for 0.8- μ m light).

In order to discuss the efficiency of Thomson scattering in more detail, let us establish a theoretical framework to show how the electron bunch duration influences the scattering efficiency. Consider a single electron slab moving with a positive velocity $V > 0$ in the laboratory frame K . Assuming the electron bunch thickness to be d' in the K' frame, in which the bunch is at rest, in the K frame, the thickness becomes: $d = d'/\gamma$, where $\gamma = (1 - V^2/c^2)^{-1/2}$.

The seed pulse, with frequency ω in the K frame, counterpropagates with respect to the electron bunch. In the K' frame, the Doppler shifted frequency equals $\omega' = \omega(1 + V/c)\gamma$ both for seed and reflected waves. In the K frame, the reflected wave frequency is larger due to the double Doppler effect: $\omega_{\text{refl}} = \omega(1 + V/c)^2\gamma^2 \approx 4\omega\gamma^2$.

Correspondingly, the electron bunch form factor in the K' frame of reference is larger:

$$k'd' = kd(1 + V/c)\gamma^2 \approx k_{\text{refl}}d/2. \quad (1)$$

Assume that the electron bunch consists of $N \gg 1$ particles with a Gaussian distribution $Nn(x')$ along the x' coordinate and a uniform distribution across a channel of cross section S , where $n(x') = (1/\sqrt{\pi}d') \times \exp[-(x'/d')^2]$ and $\int dx'n(x') = 1$, so that the probability for any given electron to have the value of x' coordinate in the interval of $(x', x' + dx')$ is equal to $n(x')dx'$. We use here the K' frame of reference which moves with the electrons and in which the Thomson scattering is free of relativistic sophistications. The result is then applied in the laboratory frame of reference using Eq. (1).

The counterpropagating electromagnetic seed wave has a spatial phase factor, $\mathbf{E}_0 \exp(-ik'x')$. Consider the amplitude of the backward scattered wave. An electron located at $x' = x_i$ is driven by the wave with a phase factor of $\exp(-ik'x_i)$. Multiplying the phase factor of the radiated wave $\exp(ik'x' - ik'x_i)$ by the phase factor of the driving force, we find that the resulting input to the electric field of the reflected wave, from all the electrons, is proportional to the following sum: $\mathbf{E} \sim \mathbf{E}_0 \sum e^{ik'x' - 2ik'x_i}$, the overall reflection coefficient being: $\eta = \mathbf{E}\mathbf{E}^*/\mathbf{E}_0^2 \sim \epsilon \sum \sum e^{-2ik'(x_i - x_j)}$. In the latter formula, the dimensionless factor ϵ is on the order of σ_T/S , where $\sigma_T = 6.6 \times 10^{-25} \text{ cm}^2$ is the Thomson cross section and the channel cross section should be as small as possible, but cannot be less than k^{-2} , thus $\epsilon \leq 10^{-16}$.

Averaging the double sum gives:

$$\eta \sim \epsilon [N + N(N-1)e^{-2(k'd')^2}]. \quad (2)$$

The difference in magnitude between the first term ($\sim N$) and the second one ($\sim N^2$) in Eq. (2) can be quite large, but only in the case where the second term does not vanish due to the exponential factor $e^{-2(k'd')^2}$. Thus the condition for highly efficient backward scattering ($\eta \sim 1$) appears to be as follows: $N > \min(\epsilon^{-1}, \epsilon^{-1/2}e^{(k'd')^2})$. According to the above estimate for ϵ , properly bunched ($\epsilon^{-1/2}$) $\sim 10^8$ electrons can be as efficient as uniformly distributed (ϵ^{-1}) $\sim 10^{16}$ electrons. To achieve this, one should have $k'd' \sim 1$, or, according to Eq. (1),

$$kd \sim 1/2\gamma^2. \quad (3)$$

Using shorter bunches allows shorter wavelengths to be efficiently reflected by a moderate number of relativistic electrons.

Now, to create such short electron bunches we propose the use of a second ultraintense, ultrashort laser pulse tightly focused on the entrance of a channel. We will use this ‘‘bunching’’ pulse to eject electron bunches from the channel walls and accelerate them toward the seed pulse. The channel is assumed to be a hole of diameter of $\sim 2 \mu\text{m}$ in a solid target. Such a channel has been experimentally realized [17].

To demonstrate the electron bunch generation in this channel geometry we perform 2D simulations with fully relativistic electromagnetic PIC code. The computation box is $20\lambda \times 14\lambda$, with spatial resolution 100 cells per λ . To resolve the density gradient, we take 100 electrons and 100 ions per cell. We assume the plasma to be preionized and collisionless and $Ze/m_i = e/2m_p$, as is typical for most metals.

A p -polarized bunching pulse (with its electric field in the (x, y) plane) is initiated at the left-hand boundary in vacuum and focused to a $\sim 2\lambda$ spot at the entrance of the channel. This pulse has a Gaussian profile with a duration of 10 fs (full width at half-maximum). We take the dimensionless amplitude $a_0 = 10$, thus the maximal intensity in the focus corresponds to $I = 1.37 \times 10^{18} (a_0^2/\lambda^2) \approx 2 \times 10^{20} \text{ W/cm}^2$ for $\lambda = 0.8 \mu\text{m}$. For this intensity the ion motion is still nonrelativistic and does not much influence the fast electron dynamics. The empty channel has an abrupt interface with the plasma walls, a smooth entrance, an internal diameter of 2.5λ , and a wall density of $n_0 = 25n_{cr}$. We choose $t = 0$ to be the instant when the peak of the pulse envelope reaches the channel entrance at $x = 0$. Spatial coordinates are measured in wavelengths, and time is measured in cycles.

In Figs. 1(a) and 1(b) we observe electron distributions inside and emerging from the channel. In Figs. 1(c) and 1(d) are shown the respective momentum distributions (R_x, P_x). Electron bunches with density $\sim n_0$ are observed being ejected from the plasma walls, with $\sim 1\lambda$ spacing (a). These bunches are extended in the transverse direction, but exhibit $d \ll \lambda$ thickness. The bunched electrons demonstrate fine structure (c) and approach energies of 40 MeV. On escaping the channel the electrons lose part of their energy (d), while maintaining the attosecond

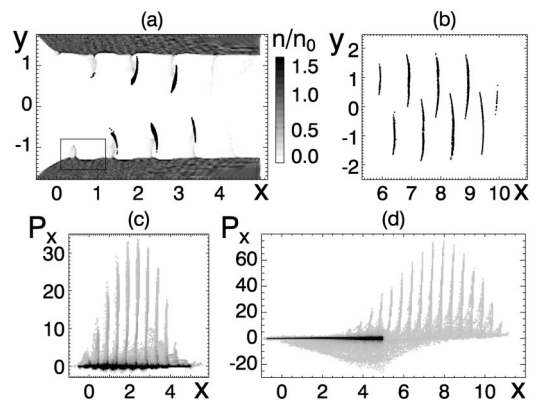


FIG. 1. Attosecond electron bunches inside, and emerging from, the channel. (a) Electron density at $t = 1$. Overlapped dots indicate electrons with energy > 10 MeV. The square indicates the jet enlarged in Fig. 3(c). (b) Positions of 20–30 MeV electrons outside the channel at $t = 9$. (c), (d) Momentum distributions of electrons corresponding to (a), (b). Simulation parameters: $a_0 = 10$, $\tau = 10$ fs, $n_0 = 25n_{cr}$.

train structure (b). The peak electron density in the bunches exiting the channel is $\sim 0.5n_0 \approx 12n_{cr}$.

To provide a more detailed view of the bunching process, free of interference from the other wall, we simulate, with the same resolution, a short tilted plasma slab with an obliquely incident (70°) 15 fs p -polarized laser pulse, focused to 1λ . A train of attosecond electron bunches and a train of attosecond electromagnetic pulses are observed emanating from the interaction. Figure 2 shows the electromagnetic energy distribution at two instants and the positions of 25–30 MeV electrons. Electrons acquire relativistic velocity in the skin layer. Having been ejected, electrons, in their turn, compress the reflected wave [2], generating the train of attosecond pulses observed in the upward direction. These electrons then move mostly along the plasma surface and the electromagnetic field provides their additional acceleration. Though the efficient generation of attosecond pulses has been found to occur under wide range of incidence angles [2,3], the attosecond electron bunch generation observed here is restricted to larger incidence angles for reasons we will discuss.

In the full 3D case, we expect the transverse bunch dimension in the z direction to be on the order of the focal diameter. Taking the $\lambda/7$ bunch thickness, for electrons above 10 MeV ($\gamma > 20$) outside the target (from the 2D simulations), and transverse bunch dimensions of $\lambda/2$ and 1λ in y and z directions, respectively, and an average density of $3n_{cr}$, we estimate the number of electrons in the bunch to be $\sim 2 \times 10^8$. According to (3), one might anticipate highly efficient interaction between a $0.8 \mu\text{m}$ seed pulse and the generated electron bunches when the bunch thickness is at least 1 order of magnitude shorter. Hence, further investigation of bunch characteristics and scattering properties is needed. It is promising to note that electrons in each 5-MeV increment above 10 MeV form sheets with thickness $\sim \lambda/30$, each containing $\sim 4 \times 10^7$ particles. This indicates a degree of order in the bunches that might be exploited to obtain a high scattering efficiency from a lower charge density.

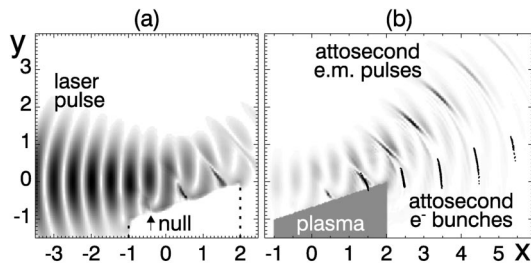


FIG. 2. Trains of attosecond electron bunches and attosecond electromagnetic pulses formed by oblique incidence on a short target. Electromagnetic energy density (gray scale): (a) $W^{1/2}$ at $t = -3$ and (b) W at $t = 3$. In (a) the arrow indicates an electromagnetic field null and in (b) overlapped black dots indicate 25–30 MeV electrons. Simulation parameters: $a_0 = 10$, $\tau = 15$ fs, $n_0 = 25n_{cr}$.

195003-3

In evaluating the efficiency of the attosecond features generated, we find that $\sim 15\%$ of an incident peak cycle has been converted to a corresponding attosecond pulse (integrating within the $1/e$ iso-intensity contour). Also, 25% has been absorbed by electrons, and among them, the bunched electrons have gained 15% of the incident pulse energy. These data demonstrate the specific mechanism of the energy conversion: the incident pulse energy is efficiently converted to the energy of attosecond electromagnetic pulses via interaction with relativistic electron bunches.

To further detail the effects of electron bunching and ejection, let us regress to a 1D model for a wave normally incident on an abrupt plasma boundary. The ponderomotive force from the incident and reflected waves acts on electrons within the skin depth [see Fig. 3(a), I]. For a sufficiently large wave amplitude this leads immediately to breaking of the stimulated Langmuir oscillations [18]. Thus, electrons from the skin layer are thrown toward the bulk of the plasma [Fig. 3(a), II]. At the same time, a counterstream of electrons arises from the bulk plasma in the direction of the skin layer [Fig. 3(a), III] due to the attractive force toward ions that were left behind by the inward-driven electrons and by the repulsive force of those electrons. The velocity of the counterstreaming electrons is relativistic. This behavior is typical of normal incidence effects, and leads to the self-intersection of electron trajectories. Near the points where the flows “stop,” e.g., $x = 0.12$, where the counterstreaming electron flow reverses to the inward-driven electron flow as observed in Fig. 3(a), III, the electron density n_e becomes very high. In maintaining a finite flux, $n_e v_e$, when the electron flow velocity v_e approaches zero, n_e must spike.

For short pulses, for pulses with a sharp tail, or even at each half-cycle of linearly polarized radiation, the elec-

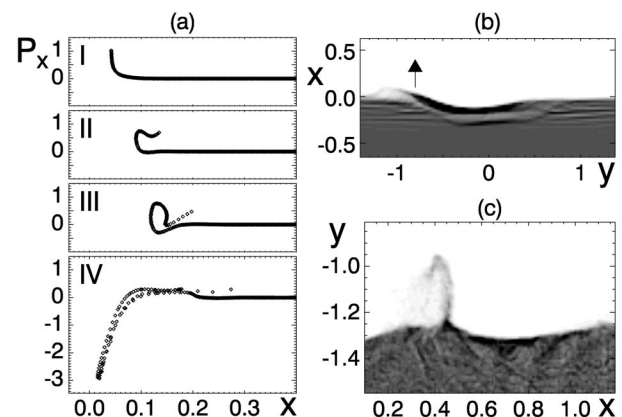


FIG. 3. Electron bunching and ejection. (a) Electron phase plane at (I–IV) $t = -0.3, -0.15, 0, 0.2$. (b) Electron density for normal incidence with $f/1$ focus at $t = 0.25$. The arrow shows electron ejection at the margin of the focus. In (a), (b) $a_{0,\text{max}} = 8$, $\tau = 2\pi/\omega_0$, $n_0 = 16n_{cr}$. Incident pulses are (a) odd and (b) even. (c) Electron jet at oblique incidence from Fig. 1(a).

195003-3

tromagnetic field, and hence, the ponderomotive force, may become zero. Under these conditions, the current of the counterstream electrons cannot be immediately switched off because of the finite system inductance. Counterstream electrons continue to flow, now with higher relativistic velocities, through the skin layer toward the vacuum, leading to a second self-intersection of electron trajectories [Fig. 3(a), IV]. The 1D model predicts that electrons will leave the plasma only to finite distances and return to the plasma [19].

Now, let us progress to a simple 2D statement of the problem, wherein tightly focused p -polarized light impinges on overdense plasma at normal incidence. Counterstreaming continues to be observed in the electrons, which may percolate through the margins of the focus [Fig. 3(b)], where $a^2 \simeq 0$, and escape the plasma. However, the best condition for electron ejection is realized when a p -polarized pulse is not only tightly focused and of short duration, but is also obliquely incident. In this case, a few effects arise: (i) the eE and $ev \times B$ forces have components which drive electrons from the skin layer into the plasma, while (ii) at the nulls of the electromagnetic field, where the laser-pulse pressure toward the wall is locally minimal [Fig. 2(a)], bulk electrons escape the plasma [Fig. 3(c)]. Furthermore, (iii) the electric field, having reversed, supports the extraction of electrons from the plasma into the vacuum, and (iv) these electrons in their turn compress the reflected radiation [2]. Thus, the electric field periodicity accounts for the $\sim 1\lambda$ periodicity of the bunches. We also find that the relativistic electrons, having been ejected by the grazing action of the p -polarized incident and reflected waves, encounter favorable conditions for further guiding and acceleration especially in the channel.

This mechanism of electron *bunching*, shown in 1D, and of electron *ejection*, shown in 2D, demonstrates, for the first time, to our knowledge, a way to generate dense attosecond electron bunches, separated from the plasma.

Attosecond electron bunch generation occurs with a range of target geometries, laser-pulse parameters, and plasma conditions, showing that our technique is *robust* and works even with a limited preplasma gradient. Because the maximal electron energy in each bunch depends on the intensity of the corresponding optical cycle, shaping of the incident laser pulse leads to shaping of the maximal energy in the electron bunch train. Consequently, the production of a *single* attosecond electron bunch is possible by reducing the incident pulse duration. Our simulations show that a focal spot of $\sim 1\lambda$ is optimal for the generation of attosecond electron bunches although larger spot sizes also work with some target geometries, at the cost of additional incident pulse energy.

In conclusion, with PIC simulations, we have demonstrated with different target geometries the efficient formation of attosecond electron bunches. The basic conditions for their generation are: p -polarization, large

angle of incidence, tight focus, short duration, and high intensity of an incident laser pulse on an abrupt overdense plasma boundary. In addition, we have derived the conditions for the efficient conversion of counterpropagating radiation into coherent x rays and its dependence on the electron bunch duration and electron energy. The suggested technique of attosecond electron bunch generation shows the promise of working with ultrashort tightly focused laser pulses from the millijoule to the joule level, applying their maximal spatial and temporal gradients to laser-plasma interaction.

The authors wish to thank the NSF (Grant No. 0114336), and the ARO (Grants No. DAAD19-03-1-0287 and No. DAAD19-03-1-0316) for their support.

*URL: <http://www.eecs.umich.edu/CUOS/attosecond>

- [1] T. Brabec and F. Krausz, *Rev. Mod. Phys.* **72**, 545 (2000).
- [2] N. M. Naumova, J. A. Nees, I. V. Sokolov, B. Hou, and G. A. Mourou, *Phys. Rev. Lett.* **92**, 063902 (2004).
- [3] J. Nees, N. Naumova, E. Power, V. Yanovsky, I. Sokolov, A. Maksimchuk, S. Bahk, V. Chvykov, G. Kalintchenko, B. Hou, and G. Mourou, *J. Mod. Opt.* (to be published).
- [4] G. Mourou, Z. Chang, A. Maksimchuk, J. Nees, S. Bulanov, V. Bychenkov, T. Esirkepov, N. Naumova, F. Pegoraro, and H. Ruhl, *Plasma Phys. Rep.* **28**, 12 (2002).
- [5] S. Bahk, P. Rousseau, T. Planchon, V. Chvykov, G. Kalintchenko, A. Maksimchuk, G. Mourou, and V. Yanovsky, *Opt. Lett.* (to be published).
- [6] S. C. Wilks and W. L. Kruer, *IEEE J. Quantum Electron.* **33**, 1954 (1997).
- [7] S. Bastiani, A. Rousse, J. P. Geindre, P. Audebert, C. Quiox, G. Hamoniaux, A. Antonetti, and J. -C. Gauthier, *Phys. Rev. E* **56**, 7179 (1997).
- [8] R. Kodama, K. Tanaka, Y. Sentoku, T. Matsushita, K. Takahashi, Y. Kato, H. Fujita, Y. Kitagawa, T. Kanabe, T. Yamanaka, and K. Mima, *Phys. Rev. Lett.* **84**, 674 (2000).
- [9] H. Ruhl, Y. Sentoku, K. Mima, K. A. Tanaka, and R. Kodama, *Phys. Rev. Lett.* **82**, 743 (1999).
- [10] Y. Sentoku, H. Ruhl, K. Mima, R. Kodama, K. Tanaka, and Y. Kishimoto, *Phys. Plasmas* **6**, 2855 (1999).
- [11] B. F. Lasinski, A. B. Langdon, S. P. Hatchett, M. H. Key, and M. Tabak, *Phys. Plasmas* **6**, 2041 (1999).
- [12] S. Baton, J. Santos, F. Amiranoff, H. Popescu, L. Gremillet, M. Koenig, E. Martinolli, O. Guilbaud, C. Rousseaux, M. Rabec Le Gloahec, T. Hall, D. Batani, E. Perelli, F. Scianitti, and T. Cowan, *Phys. Rev. Lett.* **91**, 105001 (2003).
- [13] F. Brunel, *Phys. Rev. Lett.* **59**, 52 (1987).
- [14] W. Kruer and K. Estabrook, *Phys. Fluids* **28**, 430 (1985).
- [15] R. N. Sudan, *Phys. Rev. Lett.* **70**, 3075 (1993).
- [16] E. Esarey, S. K. Ride, and P. Sprangle, *Phys. Rev. E* **48**, 3003 (1993).
- [17] S.-W. Bahk, Ph.D. thesis, University of Michigan, 2004.
- [18] V. F. D'yachenko and V. S. Imshennik, *Sov. J. Plasma Phys.* **5**, 413 (1979).
- [19] S. V. Bulanov, N. M. Naumova, and F. Pegoraro, *Phys. Plasmas* **1**, 745 (1994).